Energy, Mines and Resources Canada
Énergie, Mines et Ressources Canada

Earth Physics Branch
Direction de la physique du globe

1 Observatory Crescent
Ottawa Canada
K1A 0Y3

1 Place de l'Observatoire
Ottawa Canada
K1A 0Y3

Seismological Service of Canada

Service séismologique du Canada

GEODETIC DEFORMATION - 1946 VANCOUVER ISLAND EARTHQUAKE

William F. Slawson
Department of Geophysics and Astronomy
University of British Columbia
Vancouver, B.C.
V6T 1W5

Open File of the Earth Physics Branch Number 79-12
Ottawa, Canada
1979

26 p.

Price: $8.00

Energy, Mines and Resources Canada
Énergie, Mines et Ressources Canada

Earth Physics Branch
Direction de la physique du globe

1 Observatory Crescent
Ottawa Canada
K1A 0Y3

1 Place de l'Observatoire
Ottawa Canada
K1A 0Y3

Seismological Service of Canada

Service séismologique du Canada

GEODETIC DEFORMATION - 1946 VANCOUVER ISLAND EARTHQUAKE

William F. Slawson
Department of Geophysics and Astronomy
University of British Columbia
Vancouver, B.C.
V6T 1W5

Open File of the Earth Physics Branch Number 79-12
Ottawa, Canada
1979

26 p.

Price: $8.00

PREFACE

A recent re-examination by Rogers and Hasegawa of the available seismic data from the June 23, 1946 Vancouver Island earthquake (M_S=7.2) indicates that the earthquake was of relatively shallow (30 km or less) focal depth and the epicenter was located in central Vancouver Island rather than beneath the Strait of Georgia some 30 km or more to the east as previously thought. We have tested the Rogers-Hasegawa solution by resurveying a triangulation network in the epicentral area which had first been surveyed in 1935. The distortion of the network was found to be greater than could be accounted for by either secular strain accumulation as indicated by measurements of a nearby network or survey error but is consistent with oblique slip on a section of the Beaufort Range fault, a prominent fault that crosses the triangulation network. The best model for slip on the Beaufort Range fault involves 1.00 ± 0.25 m right-lateral and 2.50 ± 0.65 m normal slip on a shallow (0 to 5 km) segment dipping 70° NE. However, pure right-lateral slip of about 1 m over a depth interval 0 to 20 km on a vertical fault is not excluded at the 90 percent confidence limit. Thus the geodetic data support the conclusions of Rogers and Hasegawa with regard to the epicentral location and that the 1946 earthquake was caused by right-lateral motion (with or without normal slip) on the Beaufort Range fault in the vicinity of Forbidden Plateau central Vancouver Island.

PREFACE

Rogers et Hasegawa ont réexaminé récemment les données séismographiques disponibles du tremblement de terre de magnitude M_S de 7.2 survenu sur l'île Vancouver le 23 juin 1946. Ils ont conclu que le foyer est relativement peu profond, 30 km ou moins, et que son épicentre se trouve au centre de l'île Vancouver environ 30 km à l'ouest du détroit de Géorgie, où on l'avait antérieurement localisé.

Nous avons vérifié la solution de Rogers et Hasegawa en triangulant de nouveau un réseau dans la région épicentrale, qui avait été arpenté pour la première fois en 1935. Nous avons trouvé que la distorsion du réseau est plus grande que celle qu'on peut expliquer soit par les erreurs du levé ou encore par l'accumulation de tension séculaire indiquée par les mesures du réseau avoisinant. Cependant cette distorsion est compatible avec un glissement oblique le long d'une section de la faille du chaînon Beaufort, faille importante qui recoupe le réseau.

Le meilleur modèle de glissement sur cette faille comprend un décrochement dextre de 1.00 ± 0.25 m et un rejet normal de 2.50 ± 0.65 m le long d'une surface de glissement peu profond (de 0 à 5 km) à pendage nord-est de 70°. Cependant, un décrochement purement dextre d'environ un mètre le long d'une faille verticale atteignant entre 0 et 20 km de profondeur n'est pas exclus, avec une limite de confiance à 90 pour cent.

Donc, les données géodésiques appuient les conclusions de Rogers et Hasegawa quant à la localisation de l'épicentre du tremblement de terre de 1946, et aussi, quant à la nature du mouvenebt au foyer. Le séisme fut provoqué par un décrochement dextre, avec ou sans rejet normal, le long de la faille du chaînon Beaufort, à proximité du plateau Forbidden et au centre de l'île Vancouver.

TABLE OF CONTENTS

Front Cover Photograph: Line of sight from Glacier to Beecher. Glacier has more approximately 1 m northward (to the left) from its position in 1934.

Back Cover Photograph: Northwesterly view from Glacier. Dr. J.C. Savage in the foreground.

INTRODUCTION

The 1946 Vancouver Island earthquake (magnitude 7.2) was a major earthquake located within 200 km of the population centers of Vancouver and Victoria, British Columbia. A recent re-examination of existing seismic data (Rogers and Hasegawa, 1978) indicates that the epicenter was in the Forbidden Plateau region (Figure 1) of central Vancouver Island rather than beneath the Strait of Georgia some 30 km to the east as previously thought. Moreover, Rogers and Hasegawa concluded that the focal depth was not greater than 30 km, suggesting the the possibility of surface rupture. This shallow focal depth is in contrast to the 60 km focal depths for the nearby 1949 Olympia, Washington (magnitude 7) and 1965 Seattle, Washington (magnitude 6.5) events. The seismic data were not adequate to determine the mechanism of faulting uniquely but indicated some combination of right-lateral strike slip and normal dip slip on a northwest trending fault. Rogers and Hasegawa suggested the mapped Beaufort Range fault as a likely source.

The Beaufort Range fault extends in a northwest-southeast direction for more than 70 km, and the Rogers-Hasegawa epicenter lies close to the northwest end of the fault. Although the region is thoroughly dissected by linear valleys that are assumed to be faults (Muller and Carson, 1969), the Beaufort Range fault is the most prominent fault structure in the area (Figure 2). The fault brings into juxtaposition Triassic age Karmutsen volcanics and Cretaceous sediments. The stratigraphic displacement has been estimated by Muller and Carson to be about 1.5 km. No geological information is available relating to the dip of the Beaufort Range fault, but the sense of motion is readily apparent from the map prepared by Muller and Carson. To the southeast the younger rocks are on the westward side of the fault whereas in the area straddled by the triangulation net the younger rocks are to the northeast of the fault (Figure 2). The relationships place the Beaufort Range fault either in the category of a hinge fault or a left-lateral transcurrent fault. Muller (personal communication, 1978) classifies it as a hinge fault which has dropped the Cretaceous rocks relative to the Triassic rocks in the Forbidden Plateau and vice versa to the southeast.

We have tested the Rogers-Hasegawa solution by resurveying a triangulation network (Figure 2) in the epicentral area. The network, first surveyed in 1934/35, should have undergone significant distortion at the time of the 1946 earthquake if the Rogers-Hasegawa epicenter and focal depths are correct. The measured changed in the configuration of the network between 1935 and 1978 is consistent with shallow slip on the Beaufort Range fault of an amount that might be expected for a magnitude 7+ earthquake, and the precision of measurement is sufficient to exclude at the 99 percent confidence level the possibility that the measured changes are simply products of survey error.

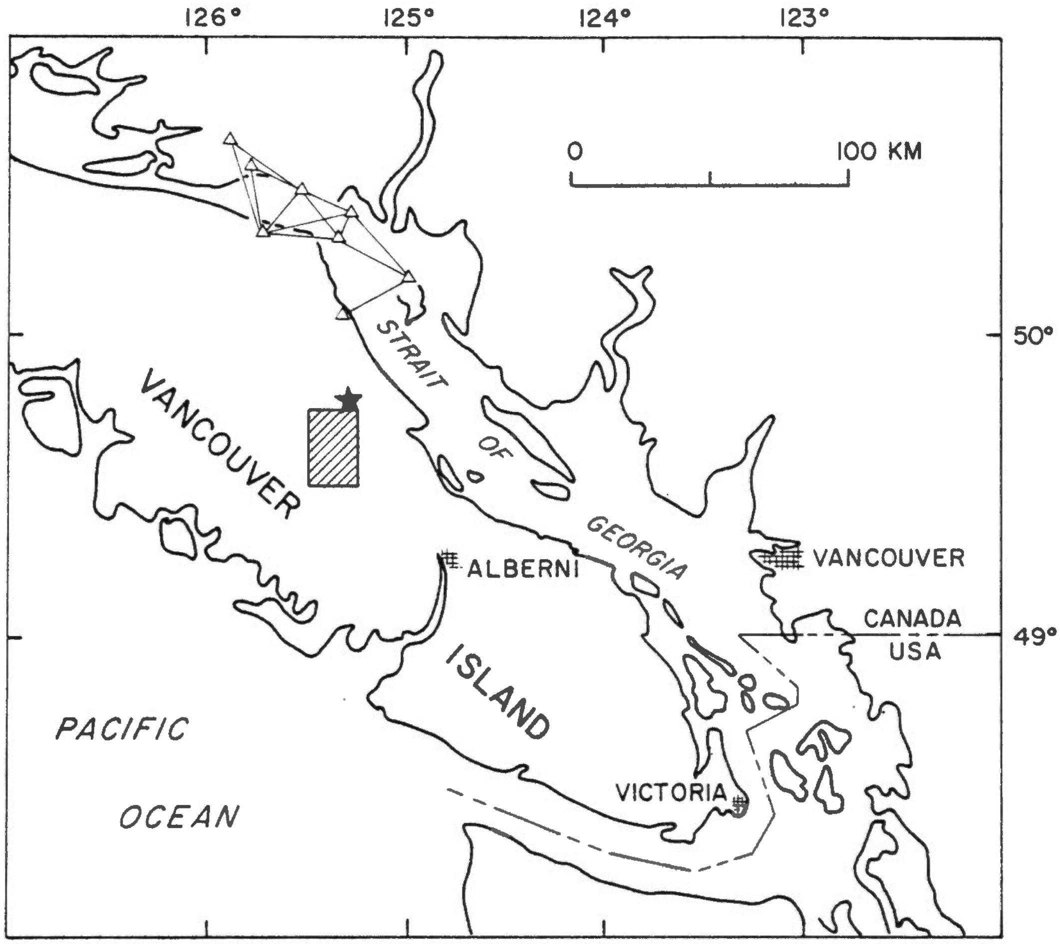

FIG. 1. Map of Vancouver Island showing the epicenter (star) of the June 23, 1946 earthquake as given by Rogers and Hasegawa (1978). The Strait of Georgia triangulation network is shown as a network of lines to the north of the epicenter. The Forbidden Plateau triangulation network likes in the shaded rectangle just south of the epicenter.

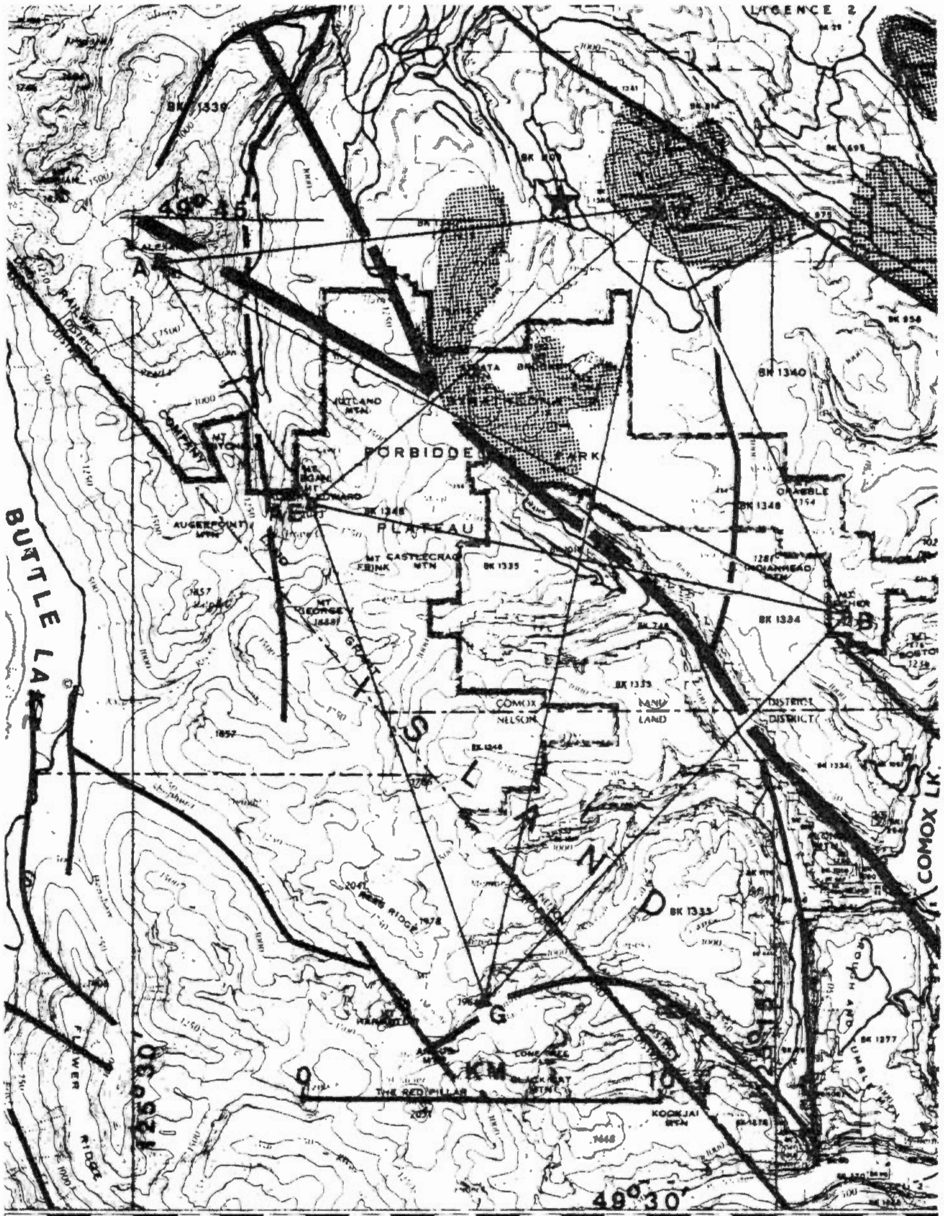

FIG. 2. The Forbidden Plateau triangulation network. The stations are identified as follows: A Alexandra, AE Albert Edward, G Glacier, W Washington, and B Beecher. The trace of the Beaufort Range fault is represented by the heavy diagonal line which passes through the network. A few of the less prominent faults are demarced by the thinner lines. The stippled areas denote Cretaceous and younger rocks whereas the remaining areas are underlain by Karmutsen formation (basalts) of Triassic or older age. The epicenter of the 1946 earthquake is indicated by a star. The location of the 15' quadrangle outlined in this figure is shown as a shaded rectangle in Figure 1. The elevation contour interval is 50 metres.

The five-station figure shown in Figure 2 is part of a large triangulation network surveyed in 1934-35 by the Surveys and Mapping Branch, Province of British Columbia. We (Figure 3) resurveyed the five-station figure in July and August 1978 to detect any angle changes which may have been caused by the 1946 earthquake. All station marks (Appendix I-V) were recovered in good condition except at Washington (W in Figure 2) where the bronze bolt had been removed from the drill hole; the 20-mm diameter drill hole in bedrock remained to identify the station (Figure 4). The accuracy of the two surveys can be judged from the root-mean-square triangle misclosure listed in Table 1 for the seven individual triangles which constitute the five-station triangulation figure.

FIG. 3. Surveyors at work

The survey consisted of turning both direct and reversed rounds at each station using a Wild T-3 theodolite. This instrument may be read directly to 0.2". A minimum of 14 rounds were turned during two occupations of each site. Signals for the three western sites (G, AE, and A) were constructed from 4"x4"x8' posts (see cover photograph), but because of the lower elevation and tree cover on the east signal lights were employed at W and B. This required those stations to be manned and the establishment of radio contact between the light tenders and instrument station. Most of the logistics within the network were handled by helicopter.

The five-station figure was adjusted by a least-squares variation of coordinates procedure for the 1934-35 and 1978 surveys separately. In the adjustments both stations W and B were held fixed. This constraint places no undue restriction upon the measured

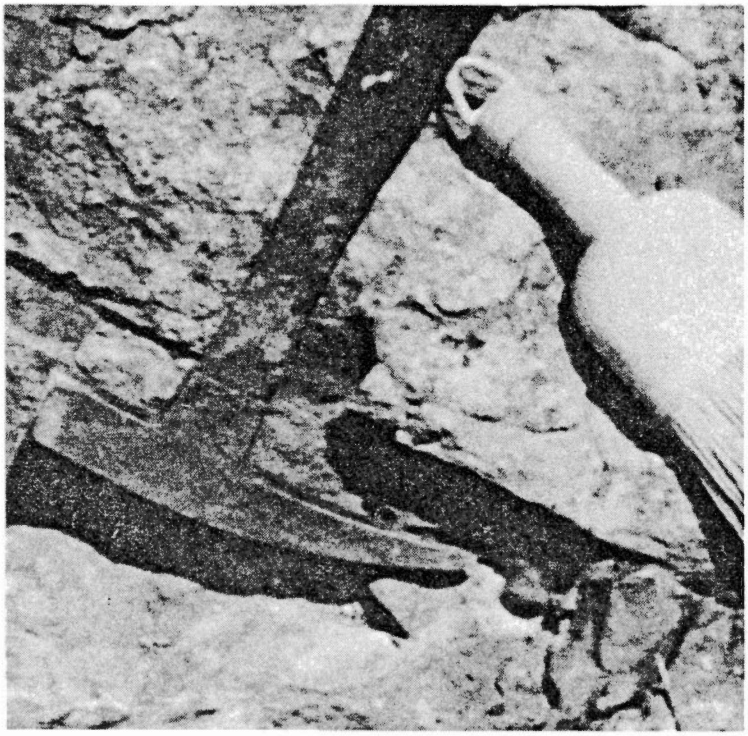

FIG. 4. Drill hole at Washington indicated by point of hammer

angles as 4 constraints are required to remove the ambiguities in rigid body displacement of the network as a whole and to resolve the ambiguity in scale. Thus, the adjustment merely requires that the angles conform to the geometric constraints of the geometric constraints of the figure (e.g. angles in a triangle must sum to 180° plus spherical excess). The maximum difference between the observed and adjusted directions was about 1.7" in each survey (Table 1). The standard deviations of an observed direction (i.e., the mean error of an observation of unit weight) as estimated from the differences between observed and adjusted directions were found to be 1.2" for the 1934-35 survey and 1.3" for the 1978 survey (Table 1). The standard deviation of an observed angle is then about 1.8" for both surveys, and the standard deviation for the difference of the 1978 and 1935 observed values of an angle is about 2.5".

TABLE 1

Statistics on accuracy of Forbidden Plateau Surveys

	Survey	
	1934/35	1978.6
R.M.S. Triangle Misclosure	2.3"	3.7"
Max. Corr. to Observed Direction	1.7"	1.6"
Std. Dev. for an Observed Direction	1.2"	1.3"
Std. Dev. for an Observed Angle	1.7"	1.9"
Std. Dev. for a Change in Observed Angle	2.5"	

Table 2 shows the difference between the 1978 measurement of an angle and its 1934-35 value for each of the 13 internal angles in the five-station network of Figure 2. A positive sign means that the angle increased during the 1935-78 interval. The differences are shown for both the observed and adjusted angles. One can test whether the observed changes in Table 2 requires that real angle changes occurred (i.e., are the observations consistent with a zero mean and 2.5" standard deviation). A chi-square test shows that the no-angle-change hypothesis can be rejected at the 99 percent confidence level. Thus real distortion of the network has been detected.

TABLE 2

Observed and adjusted angle changes between the 1934-35 and 1978 surveys and comparison of observed angle changes with those calculated for a simple Volterra dislocation model with 0.75 m right-lateral slip.

(1)	(2)	(3)	(4)	(5)	(6)
Angle	Change (1978.6-1935)			Strike-slip	Observed
	Obs*	Adj	Obs-Adj	Model	-Calc.
	"	"	"	"	"
W-A-B	0.3	-0.9	1.2	-1.7	2.0
B-A-AE	5.4	3.6	1.8	0.8	4.6
B-W-G	6.3	0.9	5.4	3.4	2.9
G-W-AE	0.2	3.1	-2.9	2.6	-2.4
AE-W-A	-1.5	-3.0	1.5	-1.3	-0.2
W-AE-B	-0.9	-3.6	2.7	-1.6	0.7
B-AE-G	-7.0	-5.2	-1.8	-3.6	-3.4
A-AE-W	1.5	0.2	1.3	2.2	-0.7
G-B-AE	-2.3	-3.3	1.0	-3.4	1.1
AE-B-A	1.6	-0.4	2.0	-1.4	3.0
A-B-W	-0.2	-0.1	0.3	-3.4	3.2
W-G-B	1.8	2.9	-1.1	4.3	-2.6
AE-G-W	8.7	5.6	3.1	2.6	6.1

*Std. dev. = 2.5"

DISCUSSION

The angle changes in Table 2 can be analyzed for shear strain accumulation by the method of Frank (1966) in the form given by Prescott (1976). This calculation assumes that the shear strain accumulated in the 1934-78 interval is uniform over the five station network in Figure 2. The angle changes in Table 2 permit one to solve for the two shear components γ_1 and γ_2. (In a coordinate system with the 1-axis directed to the east and the 2-axis to the north $\gamma_1 = e_{11} - e_{22}$ and $\gamma_2 = 2e_{12}$ where e_{ij} are the usual tensor strain components.) This resolution of shear components is particularly convenient when discussing strain across faults striking about N.45°W. as γ_1 measures right-lateral shear across such faults and γ_2 measures extension normal to such faults. The Beaufort Range fault strikes N.40°W. so the γ_1 and γ_2 components approximately resolve the strike-slip and dip-slip strain fields. The shear components calculated for the five-station network and also for the southeast quadrilateral AE-W-B-G are given in Table 3. Because the analysis of errors for the observed angle changes is somewhat more direct, we will consider here only the strain components calculated from the observed angle changes. The shear components γ_1 are marginally significant, but the shear components γ_2 do not differ significantly from zero. The total shear strains γ are marginally significant and consistent with right-lateral shear across the Beaufort Range fault (strike N.40°W.). Thus, the data indicate right-lateral slip on the Beaufort Range fault in the period 1934-78 marginally significant at the 95 percent confidence level. The standard deviations for the observed values of γ_1 and γ_2 are about twice as large as would be expected from the precision

TABLE 3

Strain components and azimuth of plane of maximum right-lateral shear for the strain accumulated in the 1935-78 interval as calculated from the observed angle changes in Table 2 and the calculated angle changes in Table 4 for the oblique-slip dislocation model. Quoted uncertainties are standard deviations.

	γ_1 μstrain	γ_2 μstrain	γ μstrain	Azimuth degrees
Observed Angle Changes	(Table 2)			
All Angles	22 ± 11	1 ± 13	22 ± 12	N46°W ± 16°
SE quadrilateral	32 ± 12	-10 ± 15	33 ± 11	N36°W ± 14°
Oblique-Slip Dislocation Model (Table 4)				
All angles	25 ± 10	1 ± 11	25 ± 10	N45°W ± 13°
SE quadrilateral	35 ± 6	-12 ± 7	37 ± 5	N35°W ± 3°

of the surveys. Presumably these large standard deviations are caused by inhomogeneous strain across the network which is not accounted for in Prescott's formulation.

We have analyzed a nearby resurveyed triangulation network to obtain an estimate of the secular strain rate on Vancouver Island. The only network available for this purpose was the Strait of Georgia network (Figure 1) that was surveyed in 1914 and 1966 by the Geodetic Survey of Canada (Jones, 1970). The shear strain accumulation rates were found to be

$$\dot{\gamma}_1 = 0.058 \pm 0.029 \ \mu\text{strain/a}$$
$$\dot{\gamma}_2 = 0.006 \pm 0.032 \ \mu\text{strain/a}$$

The quoted uncertainties are standard deviations. It is clear that $\dot{\gamma}_1$ is only marginally significant and $\dot{\gamma}_2$ does not differ significantly from zero. Thus, there is marginal evidence for right lateral shear across a vertical plane striking N.45°W. This is the strain field expected from the northwestward motion of the Pacific plate relative to the North American plate. This secular rate would contribute only 2.5 ± 1.2 μstrain and 0.0 ± 1.4 μstrain to the total values of the shear components γ_1 and γ_2 respectively for the Forbidden Plateau network shown in Table 3. Thus, the secular strain rate makes no important contribution to the strains observed in the Forbidden Plateau triangulation network.

The relative displacements between 1935 and 1978 of the geodetic stations in the five-station network of Figure 2 can be calculated from the latitudes and longitudes found for those stations in the adjustments of the two surveys. Those displacements are shown in Figure 5 by solid arrows. Because stations W and B were arbitrarily held fixed in those adjustments, three distinct additive displacement fields are possible:

1) A constant displacement added to all stations representing a translation of the network as a whole.

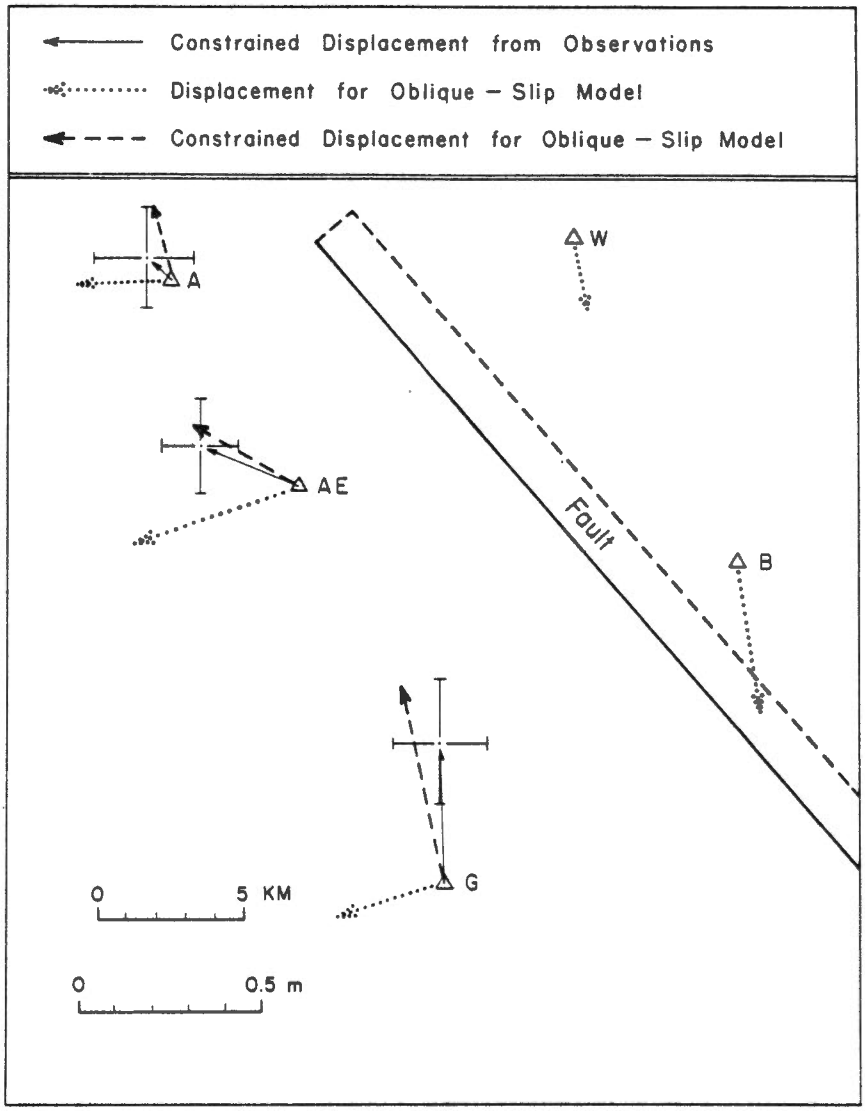

FIG. 5. Relative station displacements (solid arrows) in the Forbidden Plateau triangulation network in the epoch 1935-78 as calculated from the observed angle changes subject to the constraint that stations W and B remain fixed. The error bars represent one standard deviation on each side of the arrow head. Also shown are the unconstrained displacements (dotted arrows) calculated for the oblique-slip dislocation model and the constrained displacements (dashed arrows) calculated from the angle changes imposed by the oblique-slip dislocation model (column 4, Table 4) subject to the constraint that stations W and B remain fixed. The projection of the oblique-slip model fault upon the free surface is shown by the elongated ractangle labeled "fault".

2) Any displacement field generated by a rigid body rotation of the network as a whole.

3) An isotropic dilatation corresponding to the ambiguity in length scale.

The second and third of these displacement fields may be restricted to the rotational displacement field generated by a rigid rotation of the network about station W plus a radial displacement outward from station W that is proportional to the distance from W. The constant additive displacement is then simply the absolute displacement of station W. Notice all of these additive displacements preserve the angles in the network, the only quantities actually observed.

We have calculated the uncertainty in the displacements shown in Figure 5 by running 10 separate adjustments in which the adjusted directions were perturbed by normally distributed errors with zero mean and standard deviation 1.8" (the standard deviation expected for the difference between 1934/35 directions and 1978 directions from Table 1). The uncertainties are shown by error bars extending one standard deviation north, south, east, and west of the arrow tip representing the constrained displacements in Figure 5.

The general north to northwest trend of the constrained displacements in Figure 5 suggests right-lateral slip on the Beaufort Range fault. The decreasing displacement to the north suggests that slip on the fault may not have occurred northwest of the north end of Cruickshank canyon (7 km south of the indicated epicenter in Figure 2). To see how well strike-slip on the Beaufort Range fault could explain the observed angle changes we have modelled the rupture by a simple Volterra dislocation in an elastic half space (Chinnery 1961). The model consists of a vertical rectangular dislocation loop extending from the surface to depth D and 60 km long located so as to extend S41°E from the north end of Cruickshank canyon (Figure 6) along the trace of the Beaufort Range fault. A least-squares procedure was then used to find the amount of strike-slip most consistent with the angle changes observed in the Forbidden Plateau network. A succession of values of D (5, 10, 15, 20, 30 and 40 km) were tried, and the best fit was found for D=20 and right-lateral slip of 0.75 ± 0.24 m. The angle changes produced by such a rupture are shown in column 5 of Table 2, and the differences between the observed and calculated changes are shown in column 6. The adjusted angle changes (column 3) are more consistent with changes calculated from the dislocation model (column 5). A

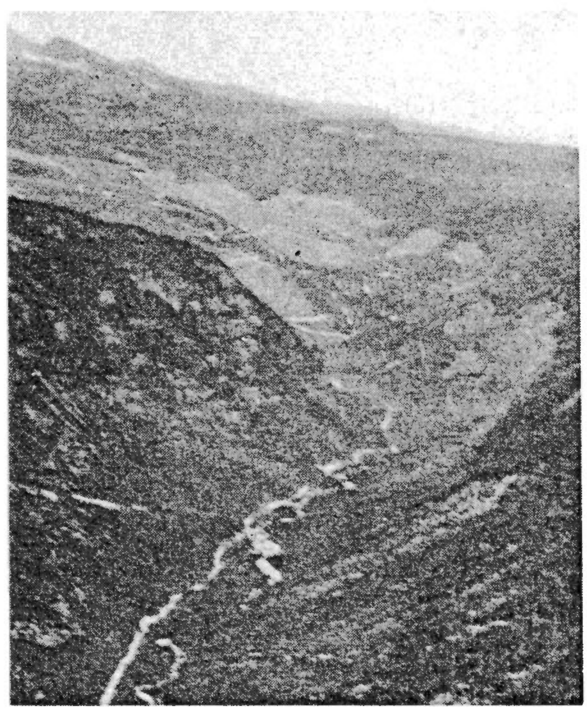

FIG. 6. Looking NW along Cruickshank canyon. The epicentral area lies near the skyline to the right of centre.

chi-square test indicates that the residuals in column 6 are consistent with calculated standard deviation of 2.5" (Table 1) for an observed angle change at about the 90 percent confidence limit. (That is, if the strike slip model were actually correct and the 1935 and 1978 observations could be repeated, the probability that the new observations would agree with theory better than the current observations would be about 90 percent.) Thus pure right-lateral slip on the Beaufort Range fault yields a barely acceptable explanation of the observed angle changes.

Much better fits to the observed angle changes were found for dislocation models representing oblique-slip on dipping faults (Mansinha and Smylie, 1971). A large number of models with different dips and downdip extent were tried. The best fit was found for 1.00 ± 0.25 m, right lateral and 2.50 ± 0.65 m nor-normal-slip on a steeply dipping (70°NE) fault extending downdip about 5 km from the surface trace of the Beaufort Range fault and extending horizontally about 60 km southeast from latitude 49°45' (the latitude of the epicenter in Figure 2) along the trace of the fault (see Figure 5). The fit of the angle changes predicted by this model to the observed and adjusted angle changes is shown in Table 4. The observed angle changes do not differ from the calculated angle changes by more than two standard deviations, and a chi-square test indicates that the model is consistent with the observations at about the 50 percent confidence limit. (Recall that agreement at the 50 percent confidence limit is the optimum result in this situation; better agreement is as

TABLE 4

Comparison of observed and adjusted angle changes between the 1934/35 and 1978 surveys with the angle changes predicted by the oblique-slip Volterra dislocation model (1.00 m right-lateral and 2.50 m normal slip on fault dipping 70°NE and extending 5 km down-dip from the surface trace of the Beaufort Range fault).

(1)	(2)	(3)	(4)	(5)
Angle	Change (1978.6-1935)		Oblique-slip	Observed
	Obs*	Adj.	Model	-Calc.
	"	"	"	"
W-A-B	0.3	-0.9	-1.3	1.6
B-A-AE	5.4	3.6	4.2	1.2
B-W-G	6.3	0.9	1.9	4.4
G-W-AE	0.2	3.1	2.9	-2.7
AE-W-A	-1.5	-3.0	-2.4	0.9
W-AE-B	-0.9	-3.6	-3.6	2.7
B-AE-G	-7.0	-5.2	-4.9	-2.1
A-AE-W	1.5	0.2	-0.5	2.0
G-B-AE	-2.3	-3.3	-4.4	2.1
AE-B-A	1.6	-0.4	-0.1	1.7
A-B-W	-0.2	-0.1	-1.1	1.3
W-G-B	1.8	2.9	3.7	-1.9
AE-G-W	8.7	5.6	5.7	3.0

* Std. Dev. for an observed angle change = 2.5"

improbable as worse agreement.) The adjusted angle changes do not differ from those predicted by the dislocation model by more than 1.1". This oblique-slip dislocation model is reasonably consistent with nodal plane solution C given by Rogers and Hasegawa (1978). The discrepancy in fault strike is about 11° and the discrepancy in seismic moment about a factor three. Both discrepancies are within reasonable limits for the quantities involved.

The oblique-slip model is also consistent with the shear strain solutions (Table 2) and displacement solution (Figure 5), both of which suggested pure right-lateral slip. In Table 3 we have compared the shear components produced by the oblique-slip model calculated from the angle changes in column 4 of Table 4 with the shear components calculated from the observed angle changes in column 2 of Table 2. The agreement is excellent. The consistency between the oblique-slip fault model and the observed solution is shown in Figure 5. In that figure the displacement fields have been calculated from the observed angle changes (column 2, Table 2) and the angle changes predicted by the oblique-slip dislocation model (column 4, Table 4) subject to the constraint that stations W and B remain fixed. (The actual displacements generated by the oblique-slip dislocation model are shown as dotted arrows in that figure.) The influence of the dip-slip component of slip is comparatively minor in the horizontal motions because of the relatively steep dip of the fault. The principal effect of the dip-slip motion would be to produce elevation changes. No data on elevation changes across the Beaufort Range fault in the epicentral area are available. Rogers and Hasegawa (1978) have discussed elevation changes possibly associated with the 1946 earthquake of up to 0.09 m near Alberni and along the coast of Vancouver Island east of the epicenter. These elevation changes are not explained by our dislocation models.

The large component of normal-slip in the oblique-slip model is to some extent at variance with the tectonic model for the Vancouver Island region as proposed by Riddihough (1977). The model suggests compression normal to the Beaufort Range fault due to the convergence of the Juan de Fuca and Explorer plates upon the North American plate. Both the seismic and geodetic evidence are clear that no reverse slip on the Beaufort Range fault occurred in 1946. The right-lateral component of slip on the Beaufort Range fault can be explained by the tectonic model as the Explorer plate has a significant component of right-lateral motion relative to the North American plate. On the other hand, the geology is consistent with normal-slip on the Beaufort Range fault if the fault dips to the northeast. Moreover, Hodgson (1946, p. 309) cited field evidence for a tectonic drop of the northeast block at Comox Lake (near the southeast end of the portion of the Beaufort Range fault shown in Figure 2). It is perhaps surprising that so large a component of normal-slip on a shallow fault did not leave an identified scarp. The answer appears (Figure 7) to lie in Hodgson's report: "There is a possibility that a disturbed fault leads down this valley [along the Beaufort Range fault], but no evidence could be obtained in such wild country."

We conclude that the triangulation data indicate at the 99 percent confidence level that significant deformation occurred in the Forbidden Plateau triangulation network between 1935 and 1978. Moreover, the deformation is consistent with about 1 m of right-lateral slip and up to 3 m of normal-slip on the Beaufort Range fault. Thus, the geodetic evidence confirms the epicentral region calculated by Rogers and Hasegawa (1978), and it seems reasonable to conclude that the 1946 earthquake was caused by shallow oblique-slip on a section of the Beafort Range fault.

FIG. 7. Looking SE along the Beaufort Range fault. The western end of Comox Lake is visible.

RECOMMENDATION

The next step should be to commission a detailed geologic/geomorphic study of the Beaufort Range fault in order to attempt to define a recurrence time for motion along the fault. Active logging and rapid erosion have probably destroyed any scarps, but lateral offset features might still be identifiable. Trenching and careful mapping of the trench wall often reveals vertical displacement which may be dated by the 14C method.

ACKNOWLEDGEMENTS

The success of this project is in no small measure due to the moral and physical support provided by the following: R. and T. Ahern, R. Ellis, B. Morrison, and P. Whaite. Special appreciation is accorded to Bob Slawson who volunteered many hours of his time toward the completion of the field work.

The project could not have been completed as expeditiously without the aid of J.C. Savage who assisted materially throughout the preliminary design, field work and analysis.

REFERENCES

Chinnery, M.A. (1961). The deformation of the ground around surface faults Bull. Seismol. Soc. Am. 51, 355-372

Frank, F.C. (1966). Deduction of earth strains from survey data, Bull. Seismol. Soc. Am. 56, 35-42.

Hodgson, E.A. (1946). British Columbia earthquake June 29, 1946, Jour. Roy. Astr. Soc. Can. 40, 285-319.

Jones, H.E. (1970). Geodetic survey measurements to determine motion in the earth's crust, in Earthquake Displacement Fields and the Rotation of the Earth, ed. by L. Mansinha, D.E. Smylie, and A.E. Beck, pp. 269-275, Springer-Verlag, New York.

Mansinha, L., and D.E. Smylie (1971). The displacement fields of inclined faults, Bull. Seismol. Soc. Am. 61, 1443-1440

Muller, J.E., and D.J.T. Carson (1969). Geology and mineral deposits of the Alberni map area, British Columbia, Geol. Sur. of Can. Paper 68-50, 35 pp.

Prescott, W.H. (1976). An extension of Frank's method for obtaining crustal shear strains from survey data, Bull. Seismol. Soc. Am. 66, 1847-1853.

Riddihough, R.P. (1977). A model for recent plate interactions off Canada's west coast, Can. Jour. Earth Sciences 14, 384-396.

Rogers, G.C., and H.S. Hasegawa (1978). A second look at the British Columbia earthquake of June 23, 1946, Bull. Seismol. Soc. Am. 68, 653-676.

APPENDIX I

Beecher (or Becher)

Station description from Survey Control Section, Ministry of the Environment, Victoria, B.C.

```
BEECHER                 34HN034   H2   V4   G   P    92F/11

49 39 00.3385   125 13 19.2606   1383.2M      6/1976

B.C.2090#56-59, B.C.2317#85-86, B.C.5108#200-201
SIT AT HP OF MT.BEECHER ABOUT 2.5 MILES NW OF
COMOX LAKE, 10 MILES WSW'LY FROM COURTENAY.
N.C.STEWART TRIANGN.1934, 9T327.
MKD.BY B.B.1-34 UNDER TRIPOD.
```

TO		AZIMUTH FROM N	METRES
~~MITLENACH~~	~~GEOD~~	~~25 24 57.02~~	~~36875.994~~
LAZO	GEOD	76 10 44.46	26807.866
GLACIER		223 11 47.77	14899.181
ALBERT EDWARD		281 42 03.02	15343.801
ALEXANDRA	NCS	296 52 12.40	21762.519
WASHINGTON		335 27 59.24	12639.541

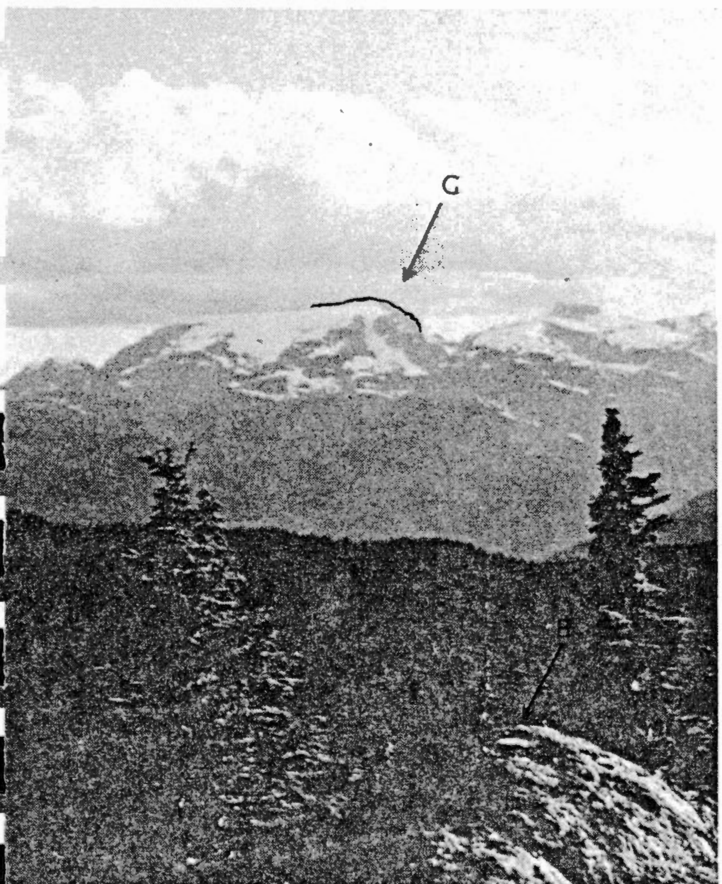

Photograph C. Line of sight
Beecher to Glacier
note: monument at lower left

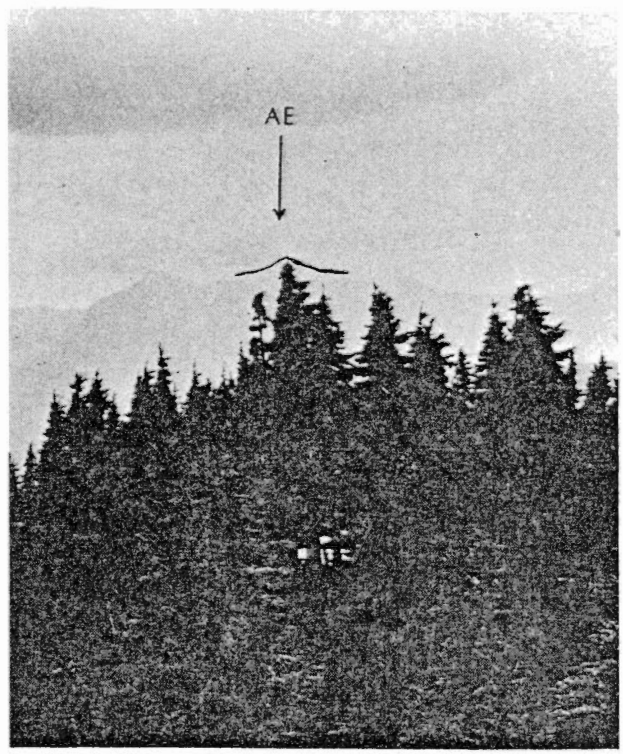

Photograph D. Line of sight
Beecher to Albert Edward

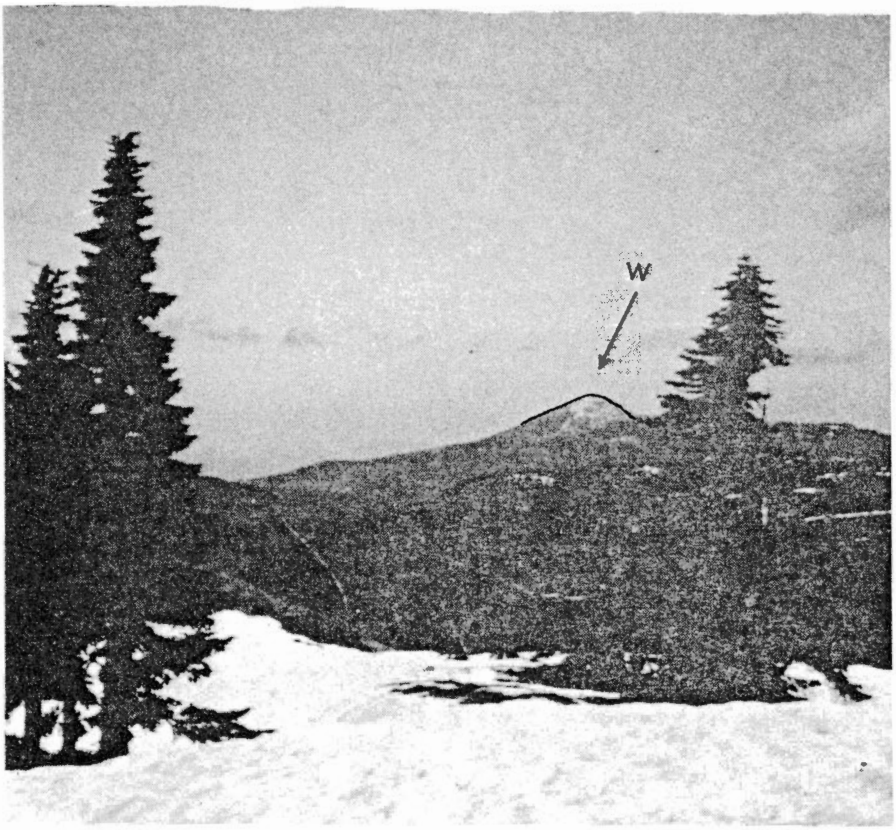

Photograph F. Line of sight
Beecher to Washington

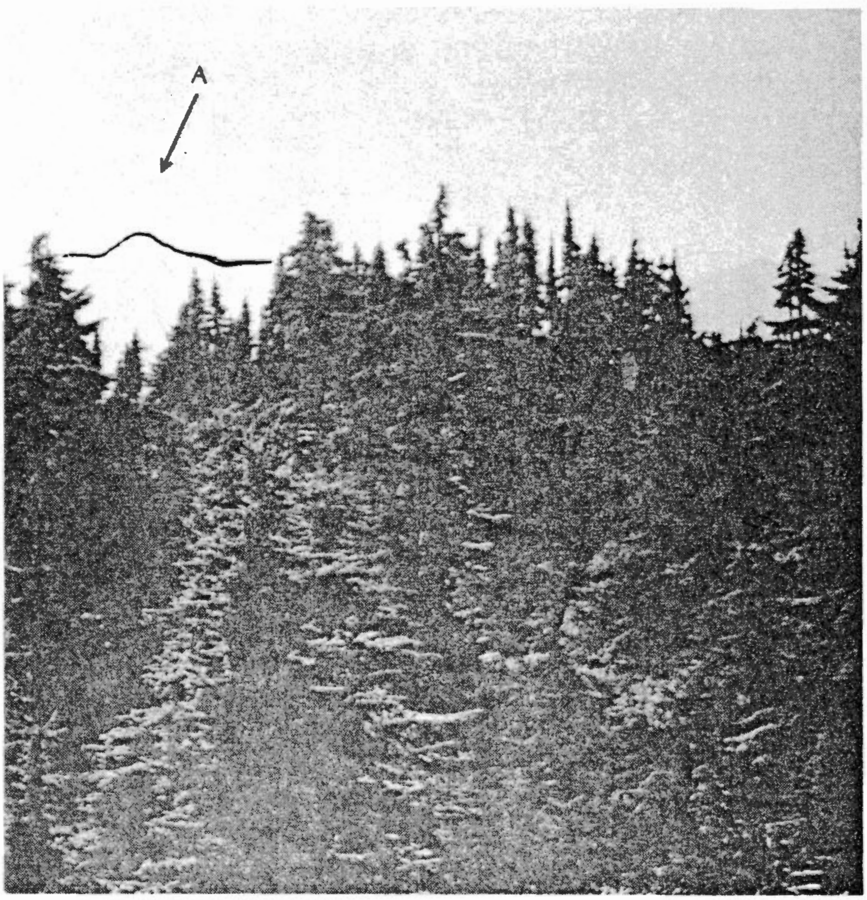

Photograph E. Line of sight
Beecher to Alexandra

APPENDIX II

Glacier

Station description from Survey Control Section, Ministry of the Environment, Victoria, B.C.

```
GLACIER              34HN048   H2   V4   G   P    92F/11

49 33 08.4613  125 21 46.6398  1964.4M     6/1976

B.C.2244#47 (NOT IDEN.)
SIT NEAR HIGHEST POINT OF COMOX GLACIER ABOUT
8 MILES W'LY FROM SOUTH END OF COMOX LAKE.
N.C.STEWART TRIANGN.1934, 9T327.
MKD.BY B.B.9-34 UNDER 5 FT.CAIRN.
```

TO		AZIMUTH FROM N	METRES
WASHINGTON		12 22 33.38	22901.472
BEECHER		43 05 21.37	14899.181
ALEXANDRA	NCS	335 53 40.07	22656.025
ALBERT EDWARD		340 50 15.66	14783.419

Photograph G. Monument
Glacier

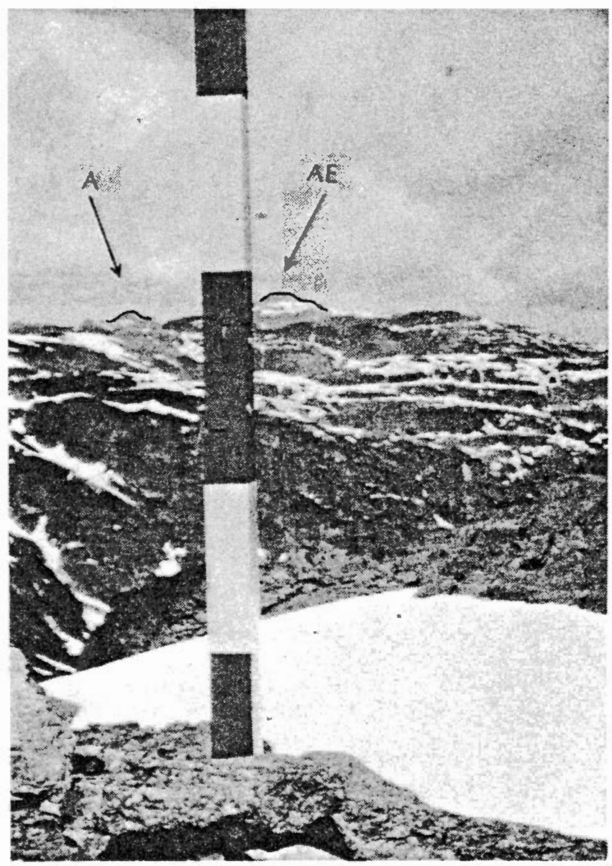

Photograph H. Line of sight
Glacier to Alexandra (not recorded)
Glacier to Albert Edward

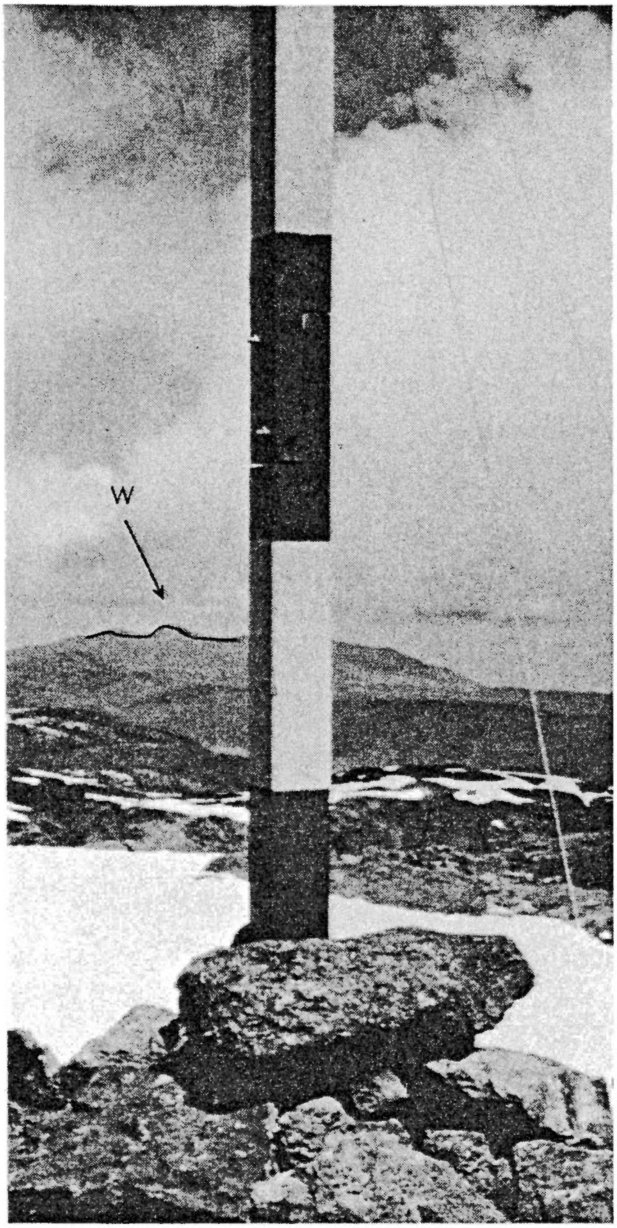

Photograph I. Line of sight
Glacier to Washington

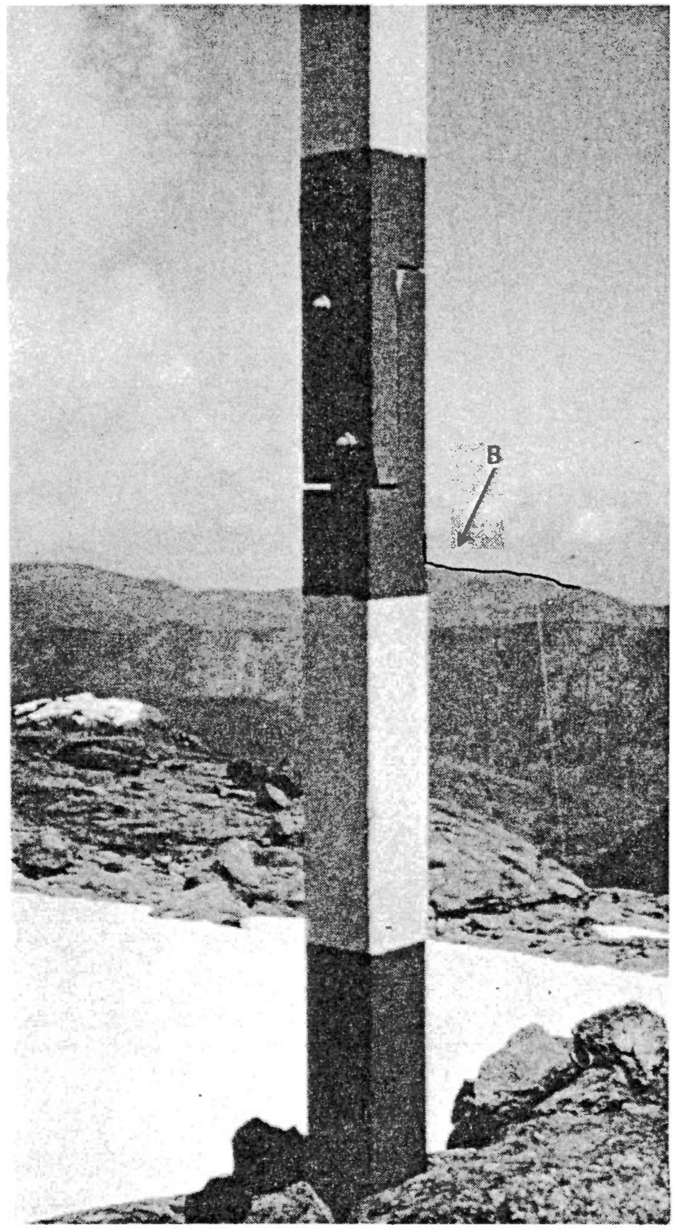

Photograph J. Line of sight
Glacier to Beecher

APPENDIX III

Albert-Edward

Station description from Survey Control Section, Ministry of the Environment, Victoria, B.C.

ALBERT EDWARD   34HN029 H2 V4 G P   92F/11

49 40 40.3846   125 25 48.6775   2093.4M   6/1976

B.C.2090#28-29, B.C.2333#17-23
SIT AT SUMMIT OF MT.ALBERT EDWARD ABOUT 5 MILES
NE'LY FROM BUTTLE LAKE NARROW AT MOUTH RALPH R.
GEOL.S.OF CAN.TRIANGN. 1910.
L.S.COKELY TRIANGN. 1926. 672/26. 5T148.
N.C.STEWART TRIANGN. 1934 & 1937. 9T327.
MKD.BY B.B.7-34 UNDER 7.5 FT.CAIRN.
TIE TO RALPH LINE CAIRNS F.B.674/26. 5T148.

TO		AZIMUTH FROM N	METRES
FORBES	1531	6 48 59.69	39581.718
GRADE		18 32 10.91	28872.197
WASHINGTON		49 13 03.02	12880.984
BEECHER		101 32 31.77	15343.801
JOAN	GEOD	128 04 11.11	47143.994
GLACIER		160 47 11.31	14783.419
BIG INTERIOR	44	203 09 42.08	26240.511
ROOSTER COMB		265 56 14.51	22826.103
MCBRIDE		287 31 26.84	16512.921
VICTORIA PEAK		311 20 05.03	63813.764
ELK		315 53 22.08	26151.216
PAUL		321 12 58.69	11243.252
ALEXANDRA	NCS	326 42 52.54	8029.285
UP.CAM.LK.LO.STA		339 52 32.63	34772.901

Photograph K. Monument
Albert Edward

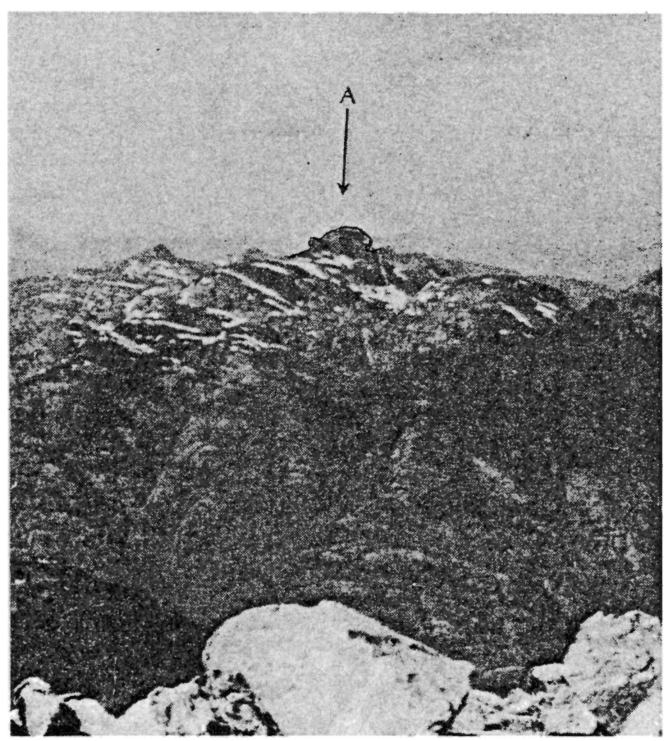

Photograph L. Line of sight
Albert Edward to Alexandra

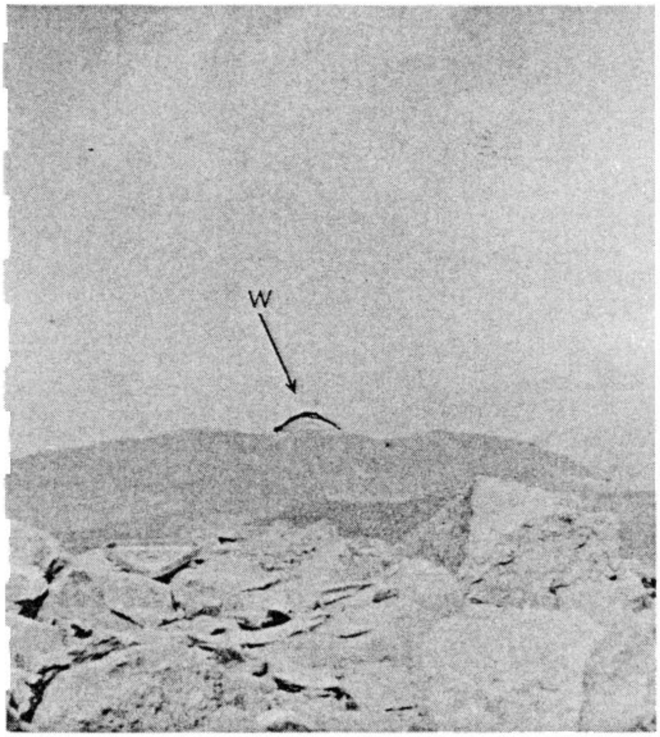

Photograph M. Line of sight
Albert Edward to Washington

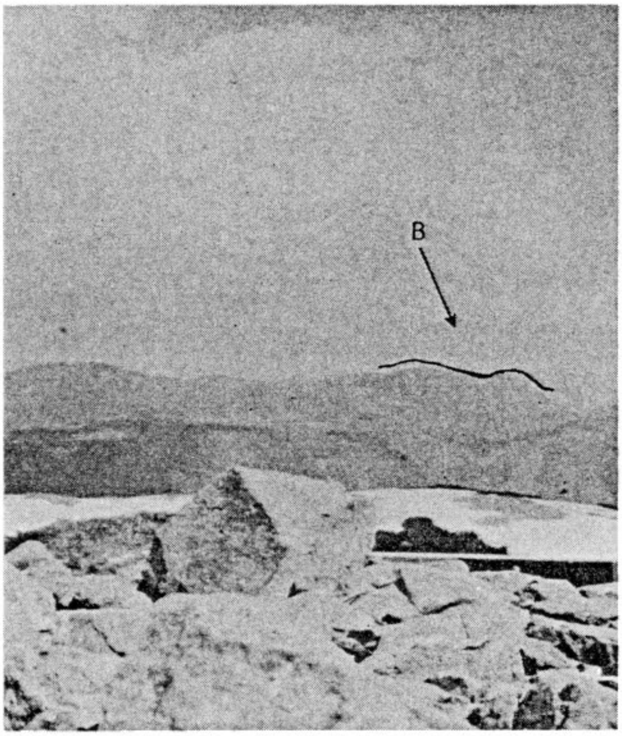

Photograph N. Line of sight
Albert Edward to Beecher

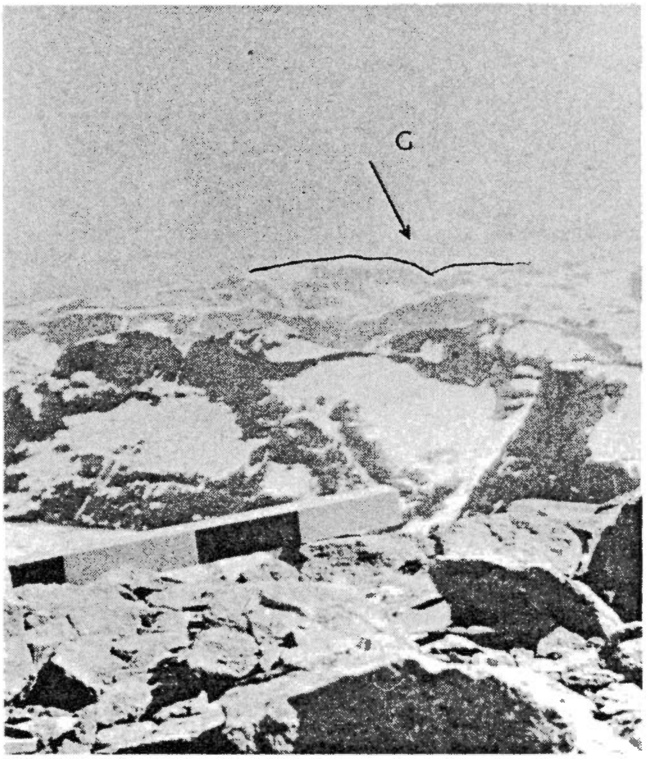

Photograph O. Line of sight
Albert Edward to Glacier

APPENDIX IV

Alexandra

Station description from Survey Control Section, Ministry of the Environment, Victoria, B.C.

ALEXANDRA NCS 34HN030 H2 V4 G P 92F/11

49 44 17.5774 125 29 28.7402 1982.1M 6/1976

B.C.2C90#31-33. B.C.2316#81-82
SIT ON THE HIGHEST AND MOST N'LY SUMMIT OF MOUNT
ALEXANDRA.(COKELYS STATION ON HORN TO SOUTH)
N.C.STEWART TRIANGN.1934. 9T327.
MKD.BY B.B.4-34 UNDER 5 FT.CAIRN.

TO		AZIMUTH FROM N	METRES
FORBES	1531	15 33 42.91	33837.728
GRADE		33 16 39.72	24728.296
GRAVEL PIT		34 06 55.94	24555.686
MITLENACH	GEOD	56 07 44.37	42340.366
WASHINGTON		83 06 02.59	14261.842
LAZO	GEOD	94 06 47.37	45573.975
BEECHER		116 39 53.07	21762.519
ALBERT EDWARD		146 40 04.69	8029.285
GLACIER		155 47 47.93	22656.025
MCBRIDE		261 13 49.98	11472.707
PAUL		307 51 19.66	3340.701
ELK		311 07 23.01	18326.959
UP.CAM.LK.LC.STA		343 42 33.18	27016.443

Photograph P. Monument
Alexandra

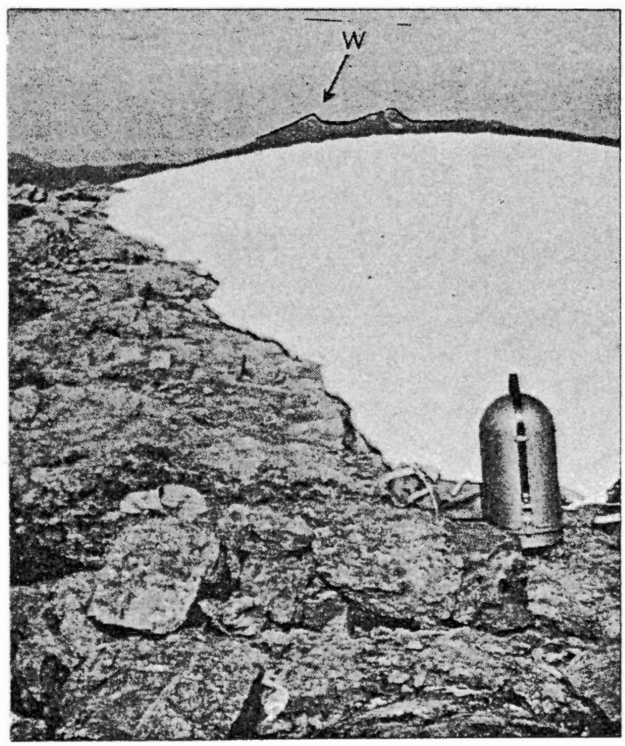

Photograph Q. Line of sight
Alexandra to Washington

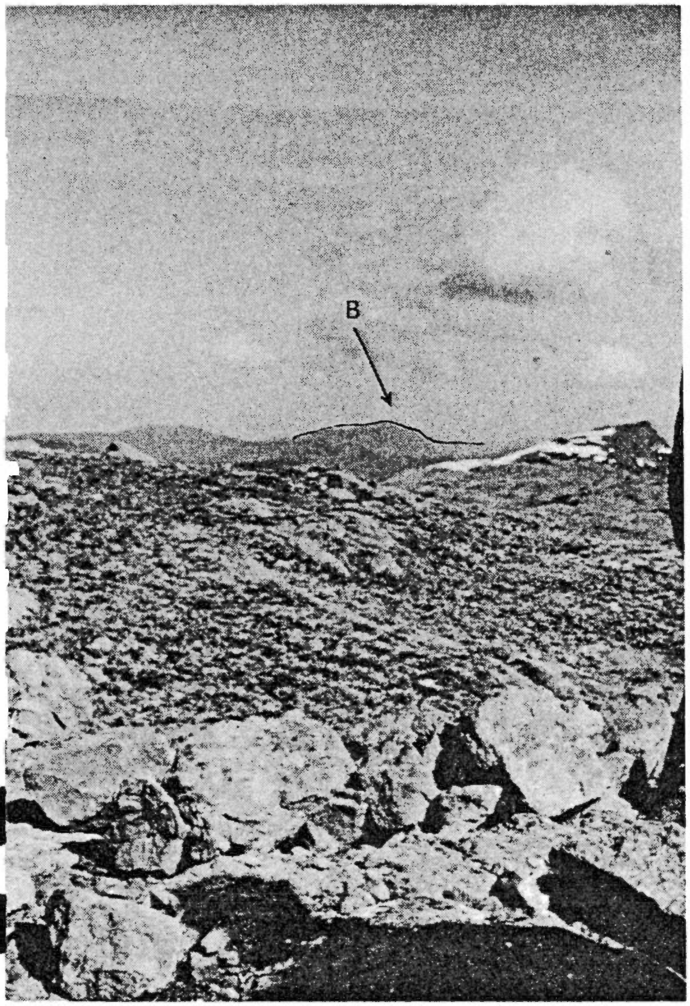

Photograph R. Line of sight
Alexandra to Beecher

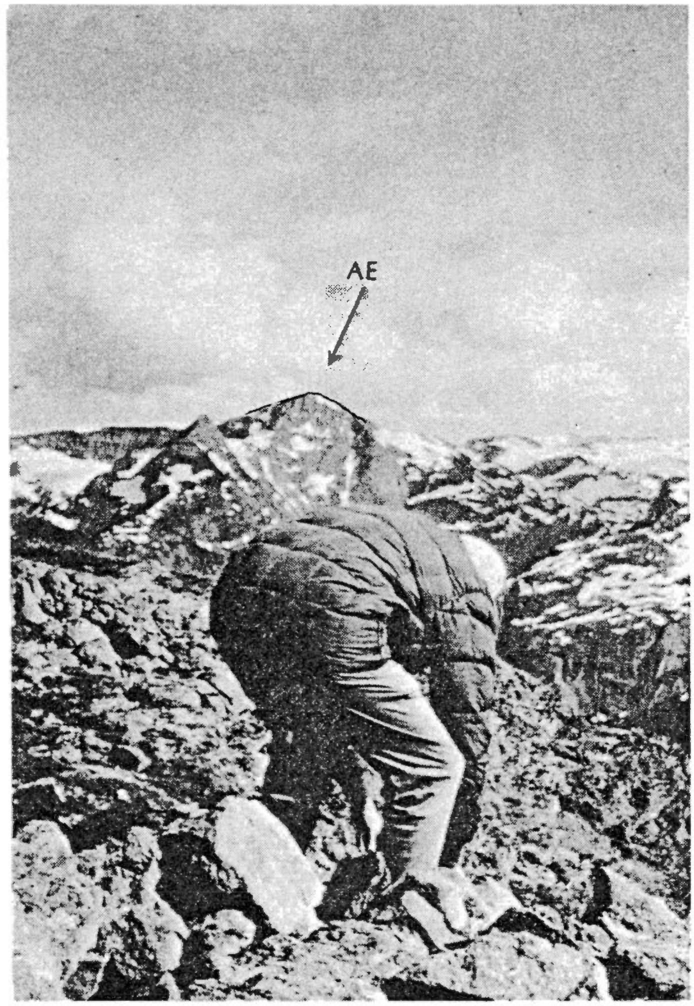

Photograph S. Line of sight
Alexandra to Albert Edward

APPENDIX V

Washington

Station description from Survey Control Section, Ministry of the Environment, Victoria, B.C.

```
WASHINGTON          34HN070   H2   V4   G   P     92F/14

49 45 12.4283   125 17 41.4404    1589.5M        6/1976

B.C.2090#53-55
SIT AT HP MT.WASHINGTON ON FORBIDDEN PLATEAU.
ABOUT 14 MILES WNW'LY FROM TOWN OF COURTENAY.
N.C.STEWART TRIANGN.1934-5. 9-10T327.
MKD.BY B.B.2-34 UNDER TRIPOD.
```

TO		AZIMUTH FROM N	METRES
GRAVEL PIT		24 29 30.62	13917.394
MITLENACH	GEOD	43 57 50.67	30327.615
LAZO	GEOD	99 11 39.86	31692.064
BEECHER		155 24 39.28	12639.541
GLACIER		192 25 40.26	22901.472
ALBERT EDWARD		229 19 14.71	12880.984
ALEXANDRA	NCS	253 15 02.39	14261.842
PAUL		271 17 56.53	16799.637
ELK		290 26 32.56	29814.684
UP.CAM.LK.LO.STA		318 14 27.56	32842.814
FORBES	1531	350 48 30.09	31299.156
GRADE		358 22 01.47	18969.348

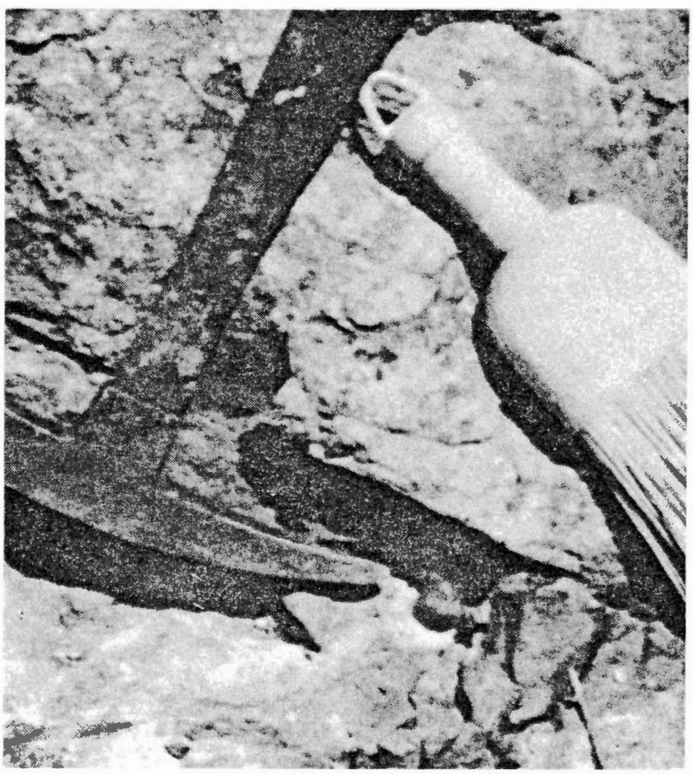

Photograph T. Monument Washington
note: Brass bolt had been removed but drill hole remained (at point of hammer).

Photograph U. Line of sight Washington to Beecher

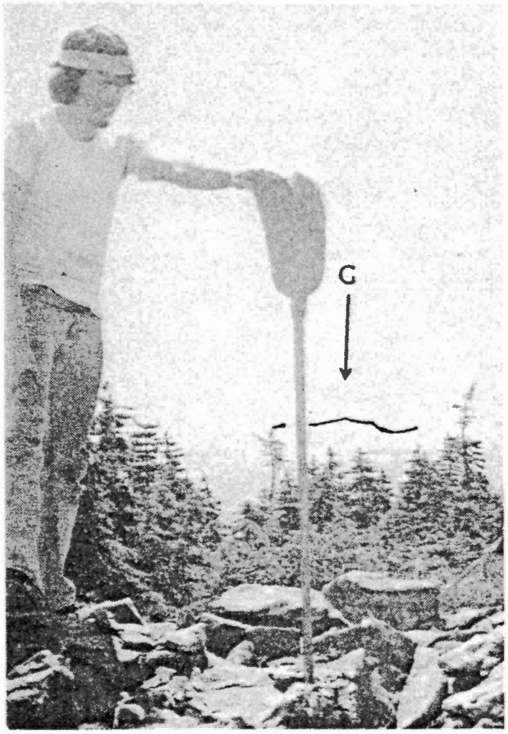

Photograph V. Line of sight
Washington to Glacier

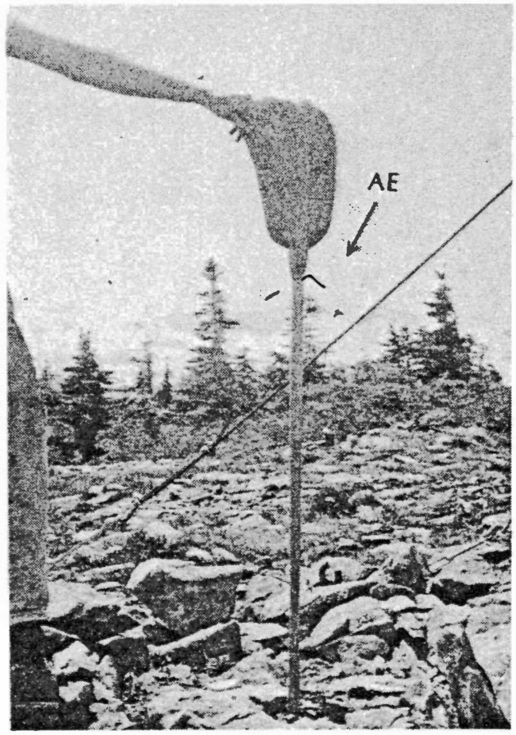

Photograph W. Line of sight
Washington to Albert Edward
note: Tree was removed.

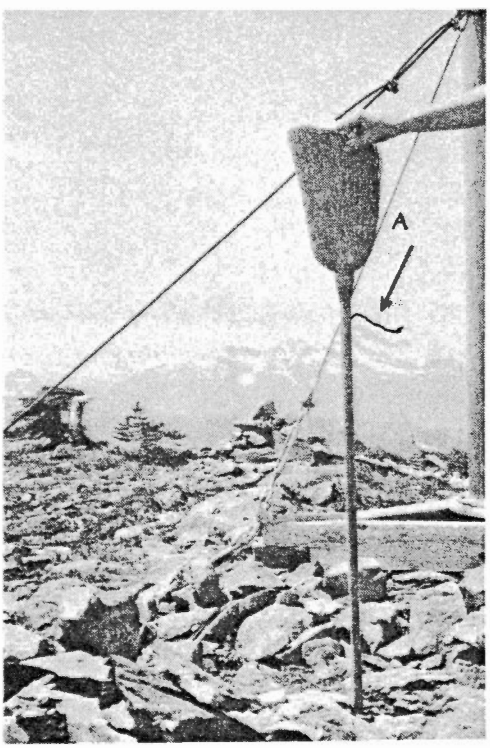

Photograph X. Line of sight
Washington to Alexandra